ANALYSIS OF GOSSANS, EXPLORATION GUIDES, AND ECONOMIC EVALUATION, POORFISH - WINDY THRUST/FOLD BELT, ENNADAI LAKE AREA, DISTRICT OF KEEWATIN

Lawrence B. Aspler
March 29, 1989

NWT GEOLOGY DIVISION - NAP
Box 1500 - Yellowknife

Indian and Northern Affairs Canada **Affaires indiennes et du Nord Canada**

EGS 1989-4 Analysis of Gossans, Exploration Guides, and Economic Evaluation, Poorfish-Windy Thrust/Fold Belt, Ennadai Lake Area, District of Keewatin
part of NTS 65 C
Canada - NWT Mineral Development Agreement;
by L.B. Aspler
1 text, 43 p.
Price: $2.20.

ABSTRACT

Numerous gossans are developed in Proterozoic supracrustal rocks (Hurwitz and Kiyuk Groups) in the Poorfish-Windy thrust/fold belt. Geochemical analyses indicate that some are anomalous in gold and arsenic. Field and petrographic data indicate that sulphide and opaque oxide minerals are epigenetic. These minerals probably grew during and after thrust-related metamorphism in the host rocks, and were probably remobilized later during brittle normal faulting. Hence the principal exploration targets are considered to be deformed and metamorphosed Proterozoic rocks adjacent to thrust faults and adjacent to late normal faults, particularly where the latter intersect the thrusts. The economic significance of the study area remains unproven. The presence of locally elevated gold values and regional gold mineralization (past-producer, Shear Lake deposit) suggest that Proterozoic supracrustal rocks in the District of Keewatin may be hosts for economic deposits. This remains to be tested by detailed mapping and prospecting in an area that has received only reconnaissance-level study.

INTRODUCTION

Mapping in the Poorfish-Windy thrust/fold belt during the 1988 field season was designed to gain a better understanding of the geology of the area in order to pinpoint potential exploration targets, and to actively prospect for economic minerals. In previous publications (Aspler, 1988; Aspler et al., 1989) essential elements of the stratigraphy, sedimentology and structure of the belt were outlined. This report is a companion paper, the purpose of which is to: 1) present petrographic and geochemical data on gossanous zones encountered and sampled during the course of mapping; 2) suggest guides for future exploration based on these data; and 3) evaluate the economic potential of Proterozoic supracrustal rocks in the District of Keewatin in general and in the Poorfish-Windy belt in particular.

Recent exploration for gold in the District of Keewatin has been concentrated primarily in Archean greenstone belts, although gold was mined from pyritic quartz veins at the Shear Lake deposit (Raman et al., 1986, Miller, 1989). Data presented herein suggest that deformed Hurwitz Group and Kiyuk Group rocks are potential gold hosts that should be considered during exploration reconnaissance.

STRATIGRAPHIC, SEDIMENTOLOGIC, STRUCTURAL AND TECTONIC SETTING

Four principal lithologic packages are exposed in the Poorfish-Windy thrust/fold belt: Archean basement (Kasba Gneiss and mafic volcanic rocks); the Hurwitz Group; the Kiyuk Group (new name, replaces Ennadai Group of Eade and Chandler, 1975; see Aspler et al., 1989); and a suite of post-Kiyuk intrusive rocks (Fig. 1, Table I). Eade (1971) correlated the mafic volcanic rocks in the study area, here considered as part of the basement complex, to those exposed at Ennadai Lake, which have been dated at 2.68 +/- .006 Ga (Chiarenzelli and Macdonald, 1986). This correlation is probably valid, although the possibility that the volcanic rocks in the study area are part of the Hurwitz Group (Happotyik member, Ameto Formation, Bell, 1970b) cannot be precluded.

Sedimentation of the post-Kinga Formation Hurwitz Group and the Kiyuk Group is interpreted to have been in a north-and northwest-migrating foredeep formed by flexural subsidence during thrust sheet loading related to collision in Trans-Hudson Orogen (Aspler et al., 1989). Cycles of sedimentation are inferred to be related to rates of thrust front migration and thrust loading; the role played by subcrustal loading (Royden et al., 1987), thermal weakening from thrusting (Kominz and Bond, 1986) and intraplate stresses (Cloetingh, 1988) is unknown. Three shallowing-upward sequences are developed; each is inferred to

represent a cycle of thrust activity to thrust quiescence (see Eisbacher, 1974, Heller et al., 1988).

In Cycle I, platformal sedimentation of supermature quartz arenites (Kinga Formation) was interrupted by passage of a peripheral bulge (sub-Ameto unconformity, Bell, 1970a; Young, 1988) and abruptly overlain by deep water siltstones, arkoses, lean iron formation and mafic igneous rocks (Ameto Formation) of the foredeep. With thrust quiescence and viscoelastic relaxation (eg. Quinlan and Beaumont, 1984, Tankard, 1986), retreat of the peripheral bulge resulted in shoaling upward and deposition of platformal cryptalgal laminates and fine-grained sediments (Watterson Formation).

In Cycle II, renewed rapid thrusting and deepening resulted in drowning of the Watterson platform and fine-grained sedimentation of the Ducker Formation, followed by arrival of the thrust front and uplift to erosional levels of sub-Tavani units on the east, concurrent with uninterrupted sedimentation on the west (sub-Tavani unconformity and Tavani Formation; Bell, 1970a). Deep water siltstones and arkoses of the "Hurwitz H" unit mark the onset of Cycle III which culminated in the arrival of basement-cored thrust sheets, an erosional front, and deposition of coarse-grained alluvium (Kiyuk Group) that was subsequently thrust/fold deformed (in part cannibalized ?) by continued migration of the thrust complex (Fig. 2).

The model remains to be tested by geochronology to establish a temporal link to events in Trans-Hudson Orogen, and by further

regional mapping to resolve uncertainties in stratigraphic correlation, structural style and sense of vergence (see Aspler et al., 1989).

ANALYSIS OF GOSSANS

Gossans were found in each of the units mapped with the exception of the Nueltin Granite. Gossan localities are indicated on Figure 3 and by UTM co-ordinate in Table II. All analyses in Table II are by neutron activation performed by Bondar-Clegg and Company Ltd., Ottawa.

The most significant results of the chemical analysis are locally elevated gold and arsenic values, primarily in samples from the Hurwitz and Kiyuk Groups. Petrographic data outlined below suggest a genetic link between thrusting, metamorphism and mineralization as well as a control by late normal cross-faults.

During mapping of the contact between the Proterozoic supracustal rocks and the Nueltin Granite (Fig. 1) we prospected for skarn-related Au, U, W, Mo, and Co mineralization reported by Charbonneau and Swettenham (1986) from southeast of the map area, with the aid of a scintillometer. No high radioactivity values or gossans were noted.

Gossans in Basement

A gossanous sample of amphibolite gneiss from the Kasba Gneiss terrane on the western margin of the map area (gossan 19, Fig. 3, Table II) displayed elevated Cr (200 ppm) and Ni (98 ppm) values typical of mafic rocks (Baragar, 1977), but only background Au.

The highest concentration of gossans in the map area is in a triangular fault-bounded wedge of basement mafic volcanic rocks on northern Windy Lake (Figs. 1 and 3). Metre-scale iron and copper sulphide and oxide zones stain the mafic volcanic rocks and silicified mafic volcanic pods. The number and size of outcrops are not large, yet each one is gossanous. Furthermore, an extensive boulder field is developed in the triangular wedge; virtually every boulder is gossanous and many are partially disaggregated from exfoliation due to intense oxide/sulphide weathering.

However, despite the visual impressiveness of the gossans, only one of the samples analysed (gossan 17) yielded anomalous gold (160 ppb). All of the mafic volcanic samples showed typical values (Baragar, 1977) of Cr (200-700 ppm), but only one was anomalous in Ni (gossan 5, 200 ppm). A silicified mafic volcanic sample was high in Ba (gossan 4A, 1,100 ppm). The principal opaque minerals in the mafic volcanics are pyrrhotite, chalcopyrite, pyrite and magnetite, with secondary marcasite and hematite (Table II).

Gossans in the Hurwitz Group

In general, gossans in the Hurwitz Group are not visually impressive, consisting of centimetre to decimetre-scale oxide/sulphide stains as disseminations, pods and fracture-fills. Three samples (from gossans 1, 12, and 20) displayed elevated gold values, but visible gold was not identified in polished thin-sections.

One argillite sample from the Ameto Formation (gossan 20) displayed a gold anomaly (100 ppb) as well as elevated Ba (400 ppm), La (100 ppm) and U (5.9 ppm); gossan 21 yielded elevated Ba (430 ppm). Metamorphic biotite and cordierite from these samples lack a preferred orientation and hence are post-kinematic; pyrrhotite and chalcopyrite replace cordierite and biotite and were thus formed before the thermal peak of metamorphism (Figs. 4A, 4B).

One meta-arkose sample from the Watterson Formation (gossan 12) was anomalous in gold (< 150 ppb) as well as arsenic (> 9,000 ppm) and tungsten (49 ppm). Pyrite, arsenopyrite and secondary marcasite are developed as inclusions within a feldspar and quartz-filled fracture that cuts the metamorphic fabric (Figs. 4C, 4D, 5). Two samples were anomalous in arsenic (gossan 2, 212 ppm; gossan 14, 918 ppm). In gossan 2, pyrite with secondary hematite is disseminated in a quartz vein that, although deformed along thrust-related fabrics, is probably related to thrusting. In general, opaque minerals in the Watterson Formation

replace randomly oriented metamorphic minerals and are hence post-kinematic and post metamorphic (Fig. 6A, Table II). Enhancement along late features is indicated by opaques lining brittle fractures that cut across grain boundaries (Figs. 6 B, 7C).

One quartz arenite sample from the Tavani Formation (gossan 1) showed anomalous gold (110 ppb), arsenic (320 ppm) and tungsten (37). In this sample, metamorphic pyrite, altered to hematite, transects detrital grains (Figs. 7 A,B).

Gossans in Kiyuk Group

The highest gold anomaly (1660 ppb) is from a sample of K1 conglomerate (gossan 3) in which pyrite and secondary hematite are developed as fracture fills that cut across thrust-related fabrics (Fig. 7D).

None of the K2 arkose samples were anomalous in gold, although two were high in Ba (gossan 6D, 1,000 ppm; gossan 16, 5,300 ppm).

Gossans in 020 Diabase

Another visually impressive gossan is exposed along a waterfall on the Red River (gossan 6, Fig. 3). A north-northeast-trending diabase dyke is in brittle fault contact with Kiyuk Group arkose. Both arkose and diabase are intensely fractured. A gossanous zone, up to 3 metres wide, is developed along the 30 metre exposure of the late cross-fault, in fault gouge, arkose

and diabase. None of the samples yielded anomalous gold although one sample of fault gouge (6C) was anomalous in arsenic (110 ppm) and high Ba values were recorded in samples of diabase (6B, 1,100 ppm) and K2 arkose (6D, 1,000 ppm).

GUIDES FOR EXPLORATION

Field observations of gossans cross-cutting primary fabrics, spatial relations with pre- and post- thrust quartz veins, gossans localized along thrust-related fabrics, and high gossan concentration along late normal cross-faults, led to the conclusion that mineralization was epigenetic and structurally controlled (Aspler et al., 1989). This conclusion is confirmed by petrographic analysis.

The first prospecting guide is toward exploration of deformed and metamorphic rocks adjacent to the thrust faults. Textural data of sulphide and opaque oxide minerals concordant with, and transecting, metamorphic porphyroblasts (Figs. 4, 6, 7) suggest that, although the possibility of early diagenetic growth cannot be ruled out, mineralization was primarily syn and post metamorphic. The most likely cause of regional metamorphism was heating due to thrust loading (eg. Karabinos and Ketcham, 1988). Heating and migration of mineralizing fluids was probably related to thrust emplacement (see Oliver, 1986). On a local level, metamorphism appears to have outlasted thrust deformation, with static growth textures predominant (eg. Fig. 4A). Yet mapping has shown that relations are more complex, typical of thrust terranes

(eg. Karabinos and Ketcham, 1988). For example, static- growth actinolite assemblages in Watterson Formation rocks at the base of the hanging wall of thrust 2 are truncated and repeated by breaching thrust fault 5 (Fig. 1).

The second exploration guide is to examine the late normal cross-faults, particularly where they intersect the thrusts. Shallow level, brittle fracture development, fluid migration and mineralization related to these faults is indicated by sulphide and secondary oxide minerals filling fractures that cut across silicate grain boundaries (eg. Fig. 7C) and by the high concentration of gossans adjacent to these faults (Fig. 3). Early thrust-related mineralization may have been remobilized along the late faults (see Romberger, 1986).

ECONOMIC EVALUATION

The economic significance of gold mineralization in the study area remains unproven. Although anomalous gold values are present, they are not remarkably high and visible gold was not identified during petrographic study. Furthermore, disseminated fine-grained gold deposits would, at present, be difficult to mine economically, given the inaccessability of the south-central District of Keewatin. However the fact remains that gold values were recorded and hence the possibilty of a potentially viable deposit cannot be discounted entirely. Further work on the gossans reported herein may prove them to be more economically

viable than would appear from the present sampling.

Regionally, the genetic relationship between gold mineralization, thrust faulting and enhancement by cross-faulting may be a useful exploration model: Miller (1989) has applied a similar model to the past-producer Shear Lake Mine in the Kognak River area. Although no direct evidence of skarn-type mineralization has been found in the present study area, reports of such mineralization (Charbonneau and Swettenham, 1986) and ongoing industry work in the Sandybeach Lake area suggest that Nueltin Granite-Proterozoic supracrustal contacts merit regional exploration.

Much of the southern District of Keewatin has been studied at a reconnaissance level only. Systematic detailed mapping and prospecting are the first steps required to test the viability of these exploration models and to evaluate the regional economic potential.

ACKNOWLEDGMENTS

This mapping and economic exploration program was supported jointly by DIAND, Yellowknife; Mineral Resources Division, Geological Survey of Canada; and Energy Mines and Resources Secretariat, Government of the NWT. I am grateful to W.A. Padgham (DIAND), A.R. Miller and C.W. Jefferson (MRD, GSC) for arranging funding. T.L. Bursey contributed substantially to the mapping. B. Hodgins assisted in the field. Advice, encouragement, discussions on economic aspects and petrographic help by A.R. Miller are gratefully acknowledged. The manuscript was critically read by A.R. Miller and C.W. Jefferson.

TABLE AND FIGURE CAPTIONS

TABLE I. Description, environmental interpretation and significance of map units, Poorfish-Windy belt (from Aspler et al., 1989).

TABLE II. Location, description and geochemical analyses of gossan samples, Poorfish-Windy belt (locality numbers refer to figure 3).

FIGURE 1. A) Location of study area with respect to Hurwitz Group and Wollaston Group exposures, Trans-Hudson Orogen and the Snowbird tectonic zone (generalized after Hoffman, 1988). B) Generalized geology, Poorfish-Windy Lake area. Thicknesses (in metres) are best estimates based on map data. See Table I for

lithologic details. (From Aspler et al., 1989).

FIGURE 2. Downplunge projection, Poorfish-Windy thrust/fold belt. Using a generalized regional plunge of 20 to the northeast and east, sections drawn through A-A'-A'', B-B` and C-C' were projected up-plunge onto D-D' (see Stockwell, 1950). Over the domain of the projection, the structure is not strictly cylindrical. (From Aspler et al., 1989).

FIGURE 3. Location of samples with geochemical analyses (Table II). UTM co-ordinates given in Table II.

FIGURE 4. A) Ameto Formation argillite with cordierite (center) and randomly oriented biotite. Opaque pyrrhotite, chalcopyrite and pyrite invade cordierite and biotite. (Plane transmitted light). B) Detail of opaque core to central cordierite porphyrblast in A; po= pyrrhotite, cpy= chalcopyrite, py= pyrite. Reflected light. C) Quartz and albite-filled vein cutting fine-grained arkose. Opaques (pyrite and magetite) fill fractures in quartz vein. Transmitted light, crossed nichols. D) Same as C), reflected light.

FIGURE 5. A) and B) Irregular fractures in Watterson Formation arkose filled with pyrite (py) blades of arsenopyrite (apy) and

secondary hematite (h). Reflected light.

FIGURE 6. A) Recrystallized cement in arkosic granulestone, Watterson Formation, of fibrous actinolite (ac), magnetite and hematite. Magnetite and hematite invade actinolite and enclose detrital grains (dg). Plane transmitted light. B) Hematite-filled fractures cut across detrital plagioclase grain in arkosic granulestone, Watterson Formation. Transmitted light, crossed nichols. C) Marcasite invading detrital grains, arkose, Watterson Formation. Transmitted light, crossed nichols. D) Same as C), reflected light.

FIGURE 7. A) Random clusters of metamorphic pyrite transect detrital quartz grains and carbonate cement, Tavani Formation quartz arenite. Transmitted light, crossed nichols. B) Detail of central grain in A); pyrite with hematite rims and internal fractures filled with hematite. Reflected light. C) Early pyrite-filled fractures cut by hematite-filled fractures, Watterson Formation arkose. Reflected light. D) Quartz vein that cuts thrust-related fabrics in conglomerate is cut by opaque (marcasite, pyrite, hematite)-filled fractures. Plane transmitted light.

REFERENCES CITED

Aspler, L.B., 1988. Geology of the Poorfish-Windy thrust/fold belt, District of Keewatin. Department of Indian Affairs and Northern Development Open File Map, EGS 1988-9.

Aspler, L.B., Bursey, T.L., and Miller, A.R., 1989. Sedimentology, structure, and economic geology of the Poorfish-Windy thrust-fold belt, Ennadai Lake area, District of Keewatin, and the shelf to foredeep transition in the foreland of Trans-Hudson Orogen. In Current Research, Part C, Canadian Shield, Geological Survey of Canada Paper 89-1C, p. 143-155.

Baragar, W.R.A., 1977. Volcanism of the stable crust. In Volcanic Regimes in Canada, edited by W.R.A. Baragar, L.C. Coleman and J.M. Hall, Geological Association of Canada Special Paper 16, p. 377-405.

Bell, R.T., 1970a, The Hurwitz Group-a prototype for deposition on metastable cratons. In: A.J. Baer (ed.) Symposium on basin and geosynclines of the Canadian Shield, Geological Survey of Canada Paper 70-40, p. 159-169.

Bell, R.T., 1970b, Preliminary notes on the Hurwitz Group, Padlei map area, Northwest Territories. Geological Survey of Canada Paper 69-52, 13p.

Bell, R.T., 1968. Preliminary notes on the Proterozoic Hurwitz Group, Tavani (55K) and Kaminak Lake (55L) areas, District of Keewatin. Geological Survey of Canada Paper 68-36, 17p.

Charbonneau, B.W., and Swettenham, S.S., 1986. Gold occurrence in radioactive calc-silicate float at Sandybeach Lake, Nueltin Lake area, District of Keewatin. In Current Research Part A, Geological Survey of Canada Paper 86-1A, p. 803-808

Chiarenzelli, J.R., and Macdonald, R., 1986. A U-Pb zircon date for the Ennadai Group. In: Summary of Investigations 1986, Saskatchewan Geological Survey, Saskatchewan Energy and Mines Miscellaneous Report 86-4, p. 112-113.

Cloetingh, S., 1988. Intraplate stresses: a new element in basin analysis. In New Perspectives in Basin Analysis, edited by K. Kleinspehn and C. Paola, Springer-Verlag, New York, p. 206-230.

Dickinson W.R., and Snyder, W.S., 1978. Plate tectonics of the Laramide Orogeny. In: V. Matthews (ed.) Laramide Folding Associated With Basement Block Faulting in the Western United States. Geological Society of America Memoir 151, p. 355-366.

Dickson, J.A.D., 1985. Diagenesis of shallow-marine carbonates. In: P.J. Brenchley, and B.P.J. Williams (eds.) Sedimentology, Recent Developments and Applied Aspects. Special Publication of the Geological Society, Blackwell Scientific, Oxford, p.173-188.

Eade, K.E., 1986. Precambrian geology of the Tulemalu Lake-Yathkyed Lake area, District of Keewatin. Geological Survey of Canada Paper 84-11, 31p.

Eade, K.E., 1974. Geology of Kognak River area, District of Keewatin, Northwest Territories. Geological Survey of Canada

Memoir 377, 66p.

Eade, K.E., 1973. Geology of Nueltin Lake and Edehon Lake (west half) map-areas, District of Keewatin. Geological Survey of Canada Paper 72-21, 29p.

Eade, K.E., 1971. Geology of Ennadai Lake map-area, District of Keewatin. Geological Survey of Canada Paper 70-45, 19p.

Eade, K.E., and Chandler, F., 1975. Geology of Watterson Lake (west half) map area, District of Keewatin. Geological Survey of Canada Paper 74-64, 10p.

Eisbacher, G.H., 1974. Molasse - Alpine and Columbian. Geoscience Canada, 1, p. 47-50.

Heller, P.L., Angevine, C.L., Winslow, N.S., and Paola, C., 1988. Two-phase stratigraphic model of foreland-basin sequences. Geology, 16, p. 501-504.

Heywood, W.W., 1973. Geology of Tavani map-area, District of Keewatin. Geological Survey of Canada Paper 72-47, 14p.

Hoffman, P.F., 1988. United plates of America, the birth of a craton: Early Proterozoic assembly and growth of Laurentia. Annual Review of Earth and Planetary Sciences, 16, p. 543-603.

Karabinos, P., and Ketcham, R., 1988. Thermal structure of active thrust belts. Journal of Metamorphic Geology, 6, p. 559-570.

Kominz, M.A., and Bond, G.C., 1986. Geophysical modelling of the thermal history of foreland basins. Nature, 320, p. 252-256.

Loveridge, W.D., Eade, K.E., and Sullivan, R.W., 1988. Geochronological studies from Precambrian rocks from the southern

District of Keewatin. Geological Survey of Canada Paper 88-18, 36p.

Miller, A.R., 1989. Highlights of gold studies in the Churchill Structural Province, Kaminak greenstone belt and Hurwitz Group, District of Keewatin, NWT. In Current Research Part C, Canadian Shield, Geological Survey of Canada Paper 89-1C, p. 127-134.

Mortensen, J.K., and Thorpe, R.I., 1987. U-Pb zircon ages of felsic volcanic rocks in the Kaminak Lake area, District of Keewatin. In: Radiogenic Age and Isotopic Studies: Report 1, Geological Survey of Canada Paper 87-2, p. 123-128.

Oliver, J., 1986. Fluids expelled tectonically from orogenic belts: Their role in hydrocarbon migration and other geological phenomena. Geology, 14, p. 99-102.

Quinlan, G.M., and Beaumont, C., 1984. Appalachian thrusting, lithospheric flexure, and Paleozoic stratigraphy of the Eastern Interior of North America. Canadian Journal of Earth Sciences, 21, p. 973-996.

Romberger, S.B., 1986. Ore Deposits #9. Disseminated gold deposits. Geoscience Canada 13, p. 23-31.

Raman, S., Kruse, J., and Tenney, D., 1986. Geology, geophsics and geochemistry of the Cullaton B-zone gold deposit, N.W.T., Canada. In: L.A. Clark (ed) Gold in the Western Shield, Canadian Institute of Mining and Metallurgy Special Volume 38, p. 307-321.

Royden, L., Patacca, E., and Scandone, P., 1987. Segmentation and configuration of subducted lithosphere in Italy: an important control on thrust-belt and foredeep-basin evolution. Geology, 15, p. 714-717.

Stockmal, G.S., Beaumont, C., and Boutilier, R., 1986. Geodynamic moels of convergent margin tectonics: transition from rifted margin to overthrust belt and consequences for foreland-basin development. American Association of Petroleum Geologists Bulletin, 70, p. 181-190.

Stockwell, C.H., 1950. The use of plunge in the construction of cross-sections of folds. Proceedings of the Geological Association of Canada, 3, p. 97-121.

Tankard, A.J., 1986. On the depositional response to thrusting and lithospheric flexure: examples from the Appalachian and Rocky Mountain basins. In Foreland Basins, edited by P.Allen, and P. Homewood, International Association of Sedimentologists Special Publication 8, p. 369-392.

Thiry, M., Ayrault, M.B., and Grisoni, J.-C., 1988. Ground-water silicifiication and leaching in sands: Example of the Fontainebleau Sand (Oligocene) in the Paris Basin. Geological Society of America Bulletin, 100, p. 1283-1290.

Wanless, R.K., and Eade, K.E., 1975. Geochronology of Archean and Proterozoic rocks in the southern District of Keewatin. Canadian Journal of Earth Sciences, 12, p. 95-114.

Young, G.M., 1988. Proterozoic plate tectonics, glaciation and iron formations. Sedimentary Geology, 58, p. 127-144.

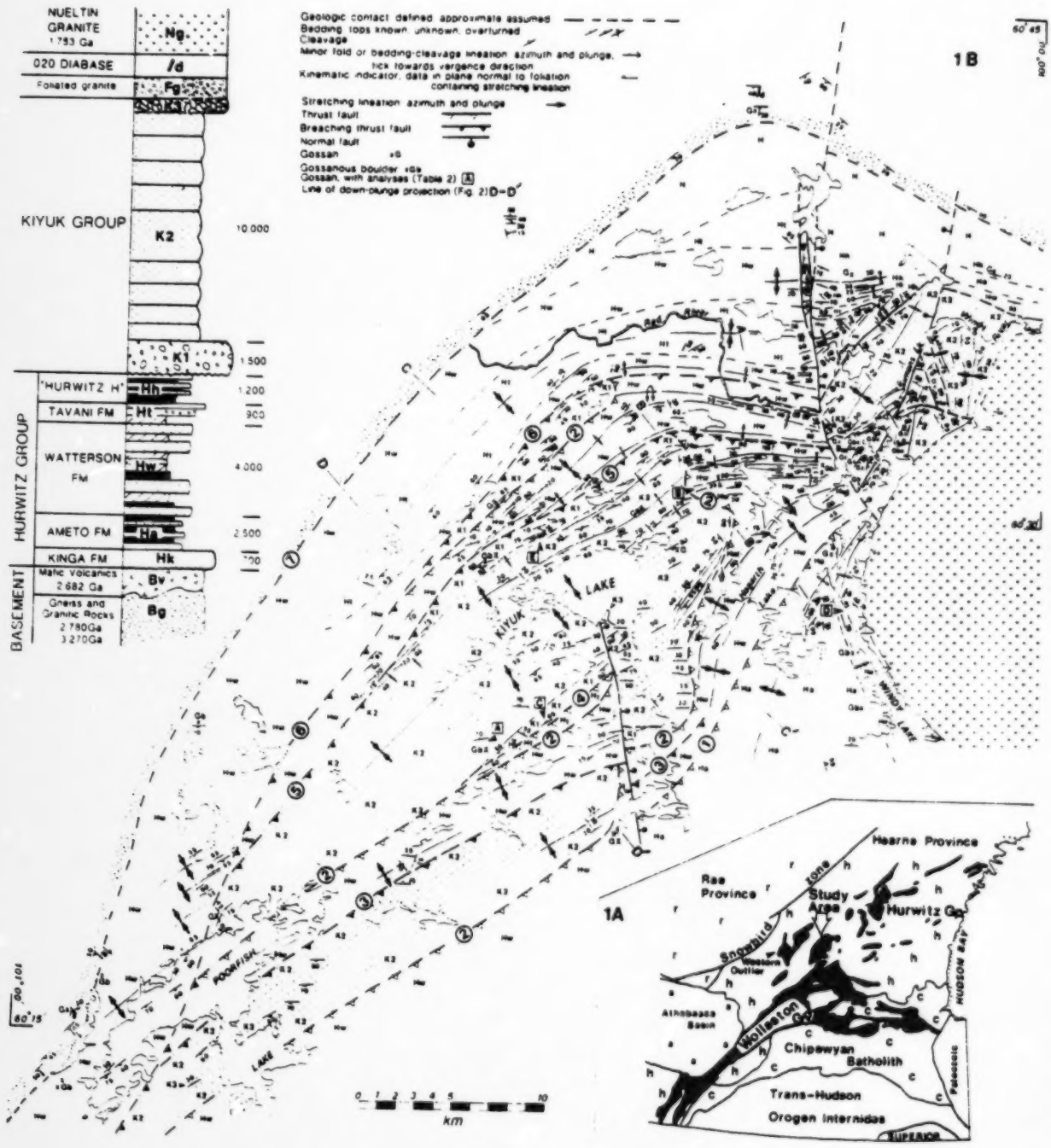

ASPLER FIGURE 1

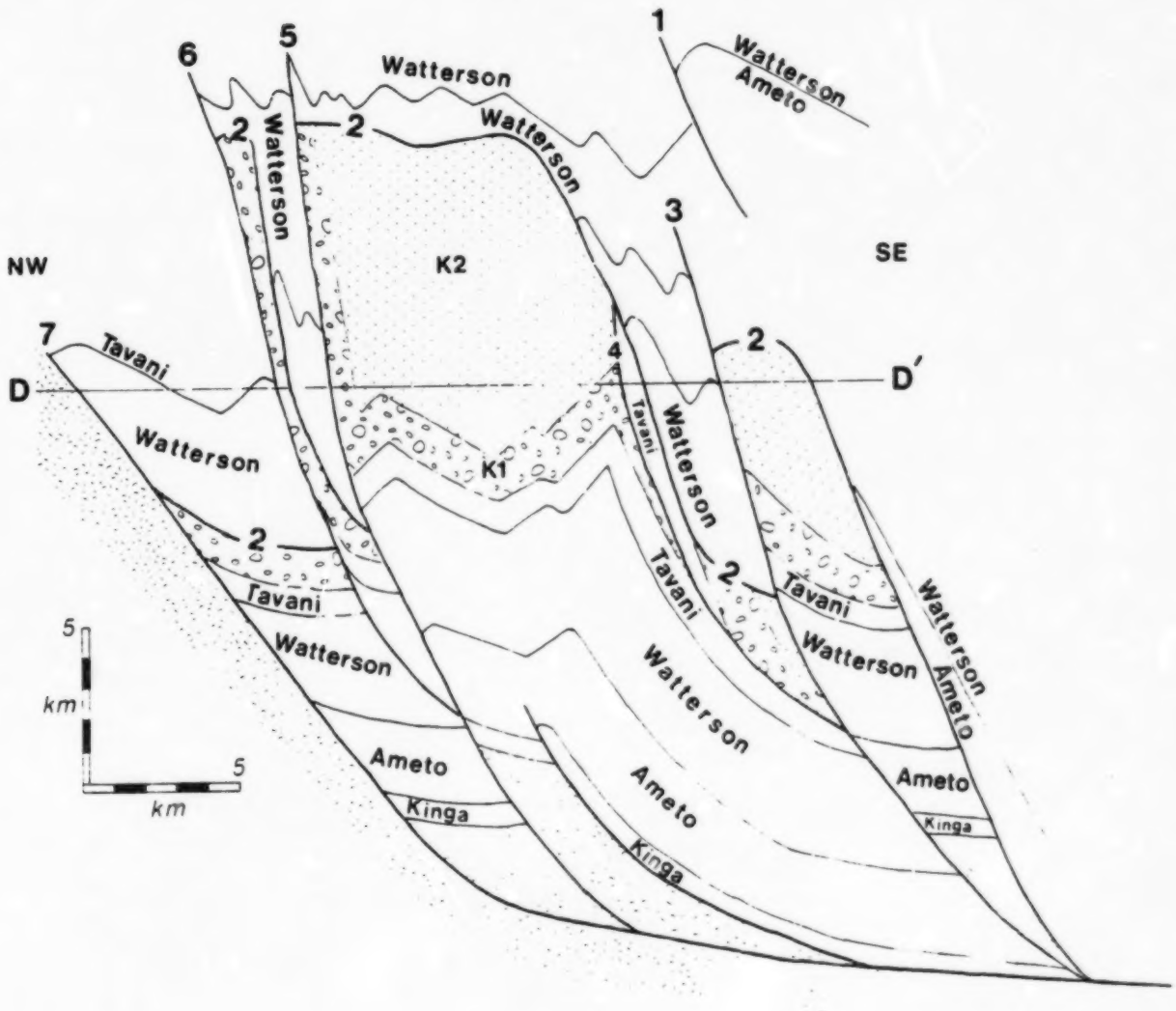

ASPLER FIGURE 2

UNIT		DESCRIPTION	INTERPRETATION	COMMENTS
Nueltin Granite		Granite, granodiorite and quartz monzonite, locally fluorite-bearing, non-foliated		U-Pb zircon 1753 + 3/-2 Ma (Loveridge et al 1988) (cf Rb/Sr Wanless and Eade, 1975)
020 Diabase		Narrow (<5 m) 020°-trending, near vertical diabase cuts basement, Hurwitz Gp and Kiyuk Group. Cuts thrust-fold fabrics, cut by NNE trending fault	Post thrust-fold deformation but pre late cross faults	Baddeleyite geochronology will be attempted
Foliated granite sill		Intrudes K2 sandstone, foliation is concordant with cleavage in adjacent sandstone	Post Kiyuk but pre-thrust-fold deformation	Zircon geochronology will be attempted
KIYUK GROUP	K3	Framework-matrix breccia with 2-80 cm angular clasts exclusively of arkose, probably derived from K2 (Fig 6D). Cemented by hematite, botryoidal quartz and tremolite-actinolite (the latter probably from a dolomitic precursor). Tabular clasts define a crude bedding	Talus, indicates cannibalization of K2, possibly due to syn-sedimentary faulting	Because of poor outcrop and structural complications it is uncertain if K3 is a separate unit above K2 or a local member within K2
	K2	Arkose with parallel stratification, low angle cross-stratification and, less commonly, wedge-planar and trough cross sets (Fig 6A, B, C). Rare pebbly beds with granitic and carbonate fragments, mudstone layers and mudchip breccias	Fluvial deposits adjacent to K1 alluvial fans. Flash floods dispersed as areally extensive, unchannelled high energy sheets with flood deceleration generally too rapid to permit the development and migration of lower flow regime bedforms	Limited paleocurrent data (Fig. 7) display high variance which may represent unchannelled flash floods spreading laterally across piedmonts. Sense of flow is opposite (westward in Kiyuk Lake, eastward north of Windy Lake) and may indicate basin segmentation during sedimentation
	K1	Massive to thickly-bedded conglomerate with local (to 3m) arkose interbeds (Fig 5). Subrounded to angular clasts up to 80 cm, clast:matrix ratios 4:6 to 9:1, framework intact and framework disrupted but generally coarse-sand matrix. 90% foliated and massive granite clasts, also with mafic volcanic, quartz arenite, carbonate, arkose, quartz-magnetite iron formation, banded sandstone-siltstone clasts	Alluvial fans with low viscosity flash flood processes predominant. Clast compositions imply basement and Hurwitz Group uplifted to erosional levels, thick conglomerate section implies significant topographic relief	Sub-K1 unconformity is not exposed in map area, all lower contacts are faults. In the western outlier supracrustal clasts are predominant (60°-) and we speculate that these may form the lower part of the section and indicate onset to basement stripping. Some outcrops mapped by Eade (1971) as part of the K1 have been reassigned to the Tavani Fm or K3
HURWITZ GROUP	Hurwitz 'H'	Siltstone, arkose and slate, siltstone to sandstone ratio varies from 7:3 to 5:5, commonly arranged in cm-dcm fining-upward cycles in the sequence erosional base to massive or graded medium grained arkose to fine grained arkose (locally parallel stratified) to siltstone (and locally mudstone) (Fig 4C, D). Rare cryptalgal laminate lenses at base	Small-scale fining upward cycles, absence of subaerial indicators suggest turbidity current like sedimentation at below wave base depths	New unit that overlies Tavani Fm in Simuris Lake Sheet (65/C-9). The name 'Hurwitz H' is used informally following Bell's (1968) alphabetical format
	Tavani Formation	Quartz arenite, conglomerate with quartz arenite and carbonate clasts, local cryptalgal laminate. In contrast to Kiyuk conglomerate Tavani conglomerate consists of quartz arenite and carbonate clasts exclusively, has a quartz arenite to calcarenite matrix, are commonly well stratified, and are not interbedded with arkose. Clasts are angular to well-rounded, granule-pebble sizes are predominant, quartz arenite to carbonate clast ratios vary from 8/2 to 2/8. Conglomerates are both framework intact and framework disrupted, matrix remains coarse sand. Cycles between components are not evident, upper contacts of cryptalgal laminates are erosional	Preliminary model of cryptalgal laminates as shallow subtidal deposits, quartz arenite as shallow water to subaereal deposits and conglomerates being intraformational, from reworking (fluvial or tidal channel migration-collapse, syn-sedimentary faulting, sea level fluctuation?) of early cemented (e.g. Dickson 1985, Thury et al. 1988) carbonates and quartz-arenites	In type area Tavani Fm is compositionally immature (Bell 1968, Heywood 1973) but in Kognak River (Eade 1974) and Tulemalu Yathkyed (Eade 1986) areas "impure quartzites" are prominent. Transition from Watterson in map area is conformable, although to the east is a basin-margin sub Tavani unconformity that cuts into progressively deeper stratigraphic levels (Bell 1970a)
	Ducker Formation	Not developed in map area (cf. Eade, 1971) greywacke and siltstone		A direct Watterson to Tavani transition is common (Eade 1974, 1986, Eade and Chandler, 1975)
	Watterson Formation	Dcm to m-scale interlayers of cryptalgal laminate and dcm-scale arkose to siltstone fining upward cycles (Fig 3C, D, E, F). Carbonate:siliciclastic ratios range from 4:6 to 9:1, carbonate rocks are generally predominant	Siliciclastic component may represent more proximal (relative to Amato) turbidite sedimentation, carbonate rocks shallow subtidal	Interlayering may represent shoaling-upward aggradational cycles the significance of which (autocyclic vs allocyclic) needs to be evaluated
	Amato Formation	Siltstone, slate, arkose. Fining upward cycles of arkose (locally graded or with parallel-stratification or small-scale cross stratification) to siltstone to mudstone (Fig 3B). Siltstone to sandstone ratio 3:7 to 1:9	Below wave base sedimentation interrupted by turbidity-like currents	Transition from supermature quartz arenites of Kinga to texturally and compositionally immature Amato appears to be abrupt. Possibility of mafic volcanic rocks in map area being Amato Fm cannot be precluded
	Kinga Formation	Snow white to pale grey weathering, fine grained quartz arenite with parallel stratification (Fig 3A)	Platform deposits, possibly multi-cyclic, and/or derived from zones of intense tropical weathering (eg Bell 1968, 1970a)	Intraformational breccia at the top of Kinga led Bell (1970a) to infer a sub-Amato unconformity
	Pethei Formation	Not exposed in map area, slate, siltstone, conglomerate, sandstone (Bell 1970a, b, Eade, 1974)		
BASEMENT		Mafic volcanic rocks with local silicification pods and possible remnant pillow selvages		2 687 ± 0059 Ga (U-Pb zircon, Chamberlain and Macdonald 1986) from northern Saskatchewan
		Thickly stratified gneiss (Kasba Lake gneiss of Loveridge et al 1988) cut by granitic rocks, granitic protomylonite		Gneiss yields to U-Pb zircon age populations of ca 3 270 and 2 780 Ga (Loveridge et al. 1988)

ASPLER TABLE I

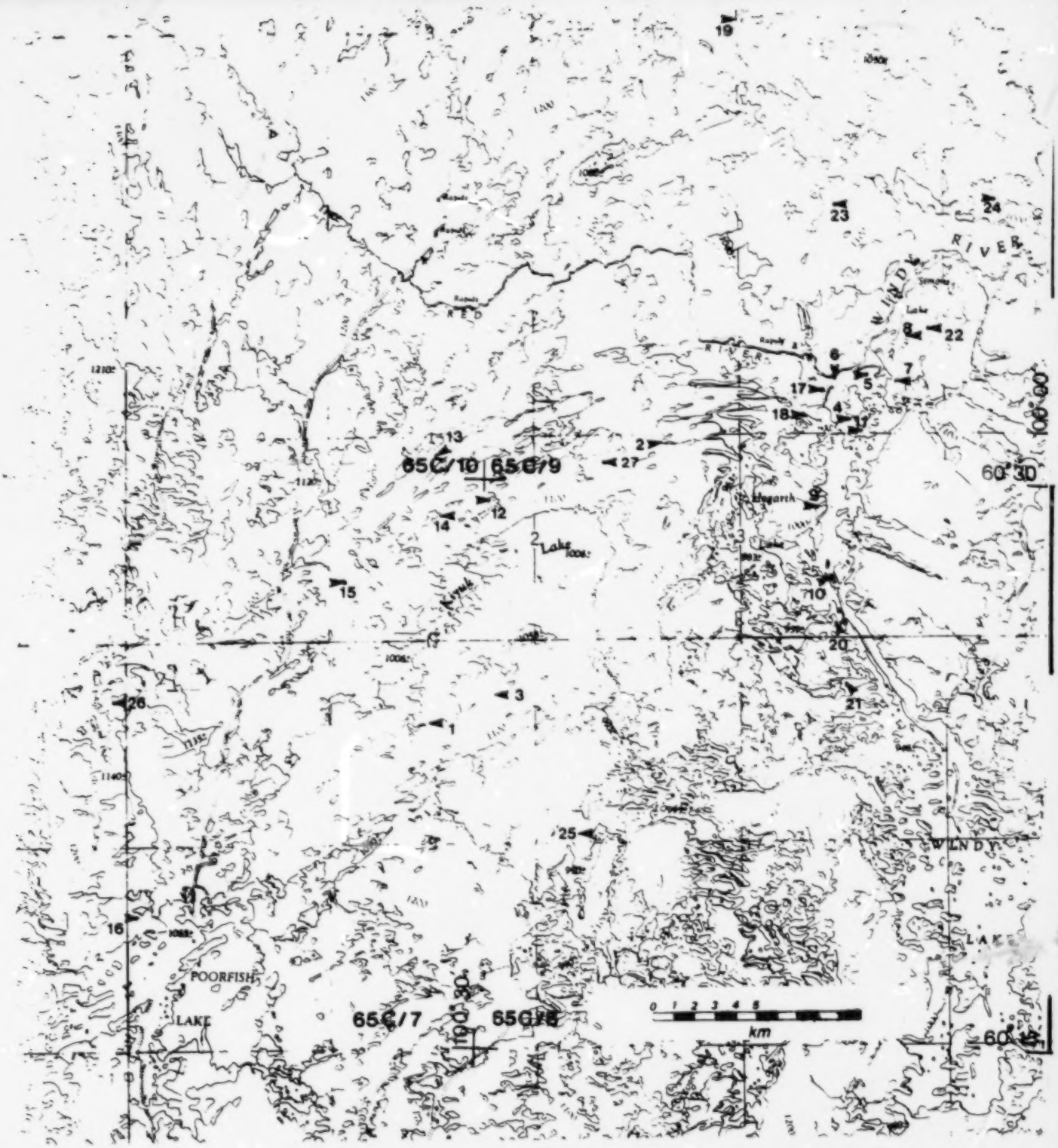

ASPLER FIGURE 3

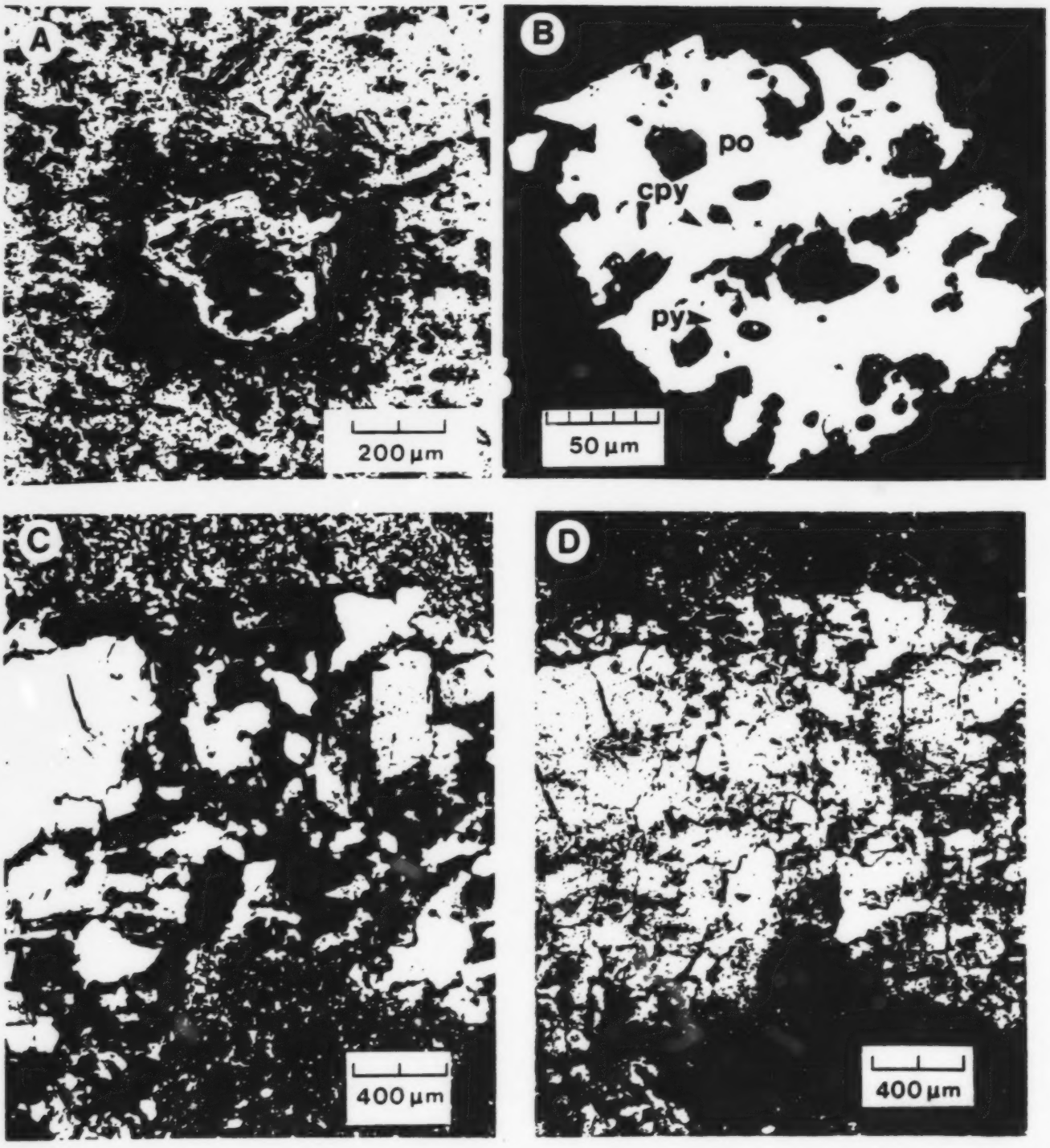

ASPLER FIG. 4

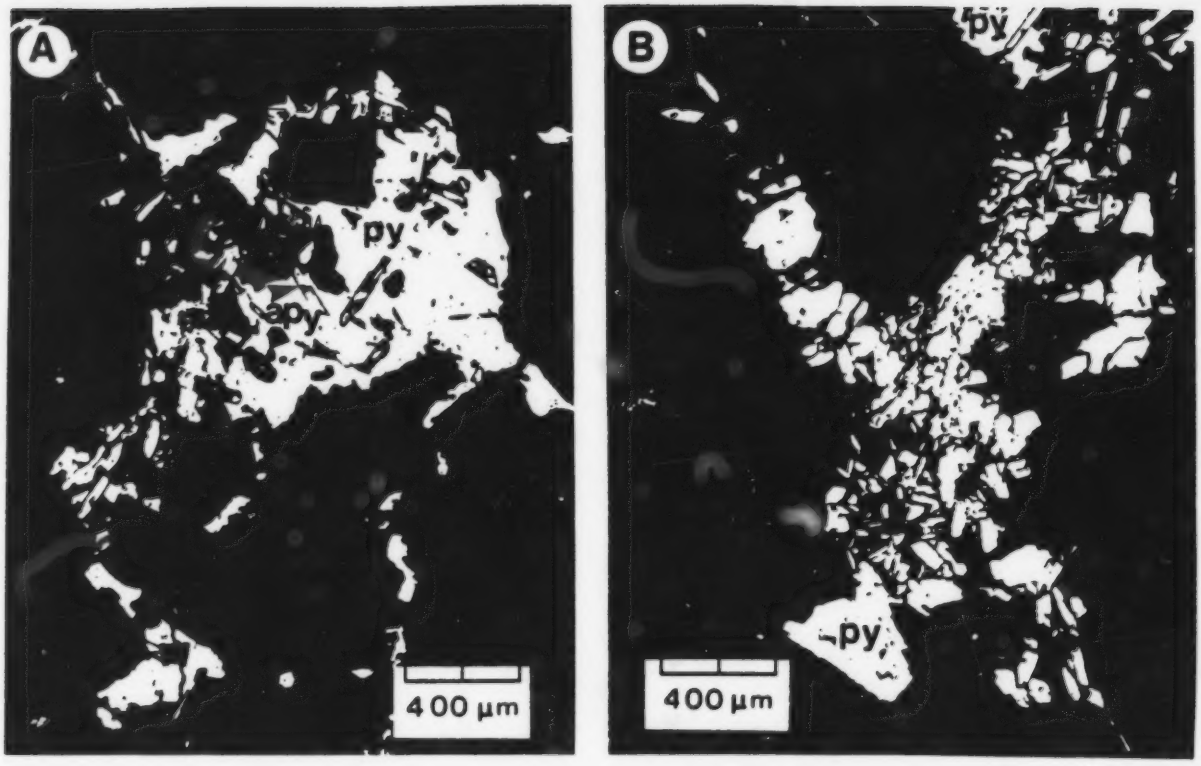

ASPLER FIG 5

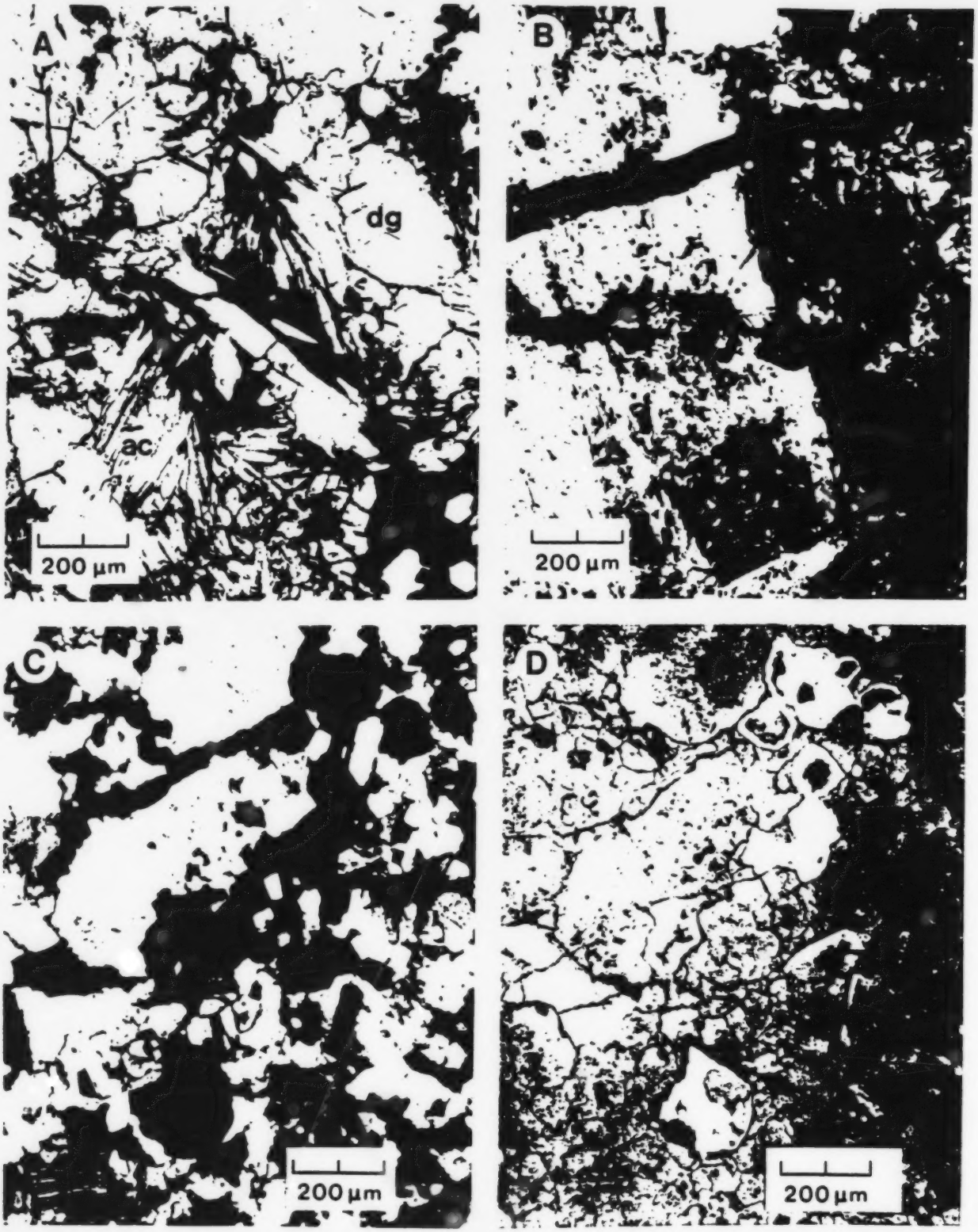

ASPLER FIG 6

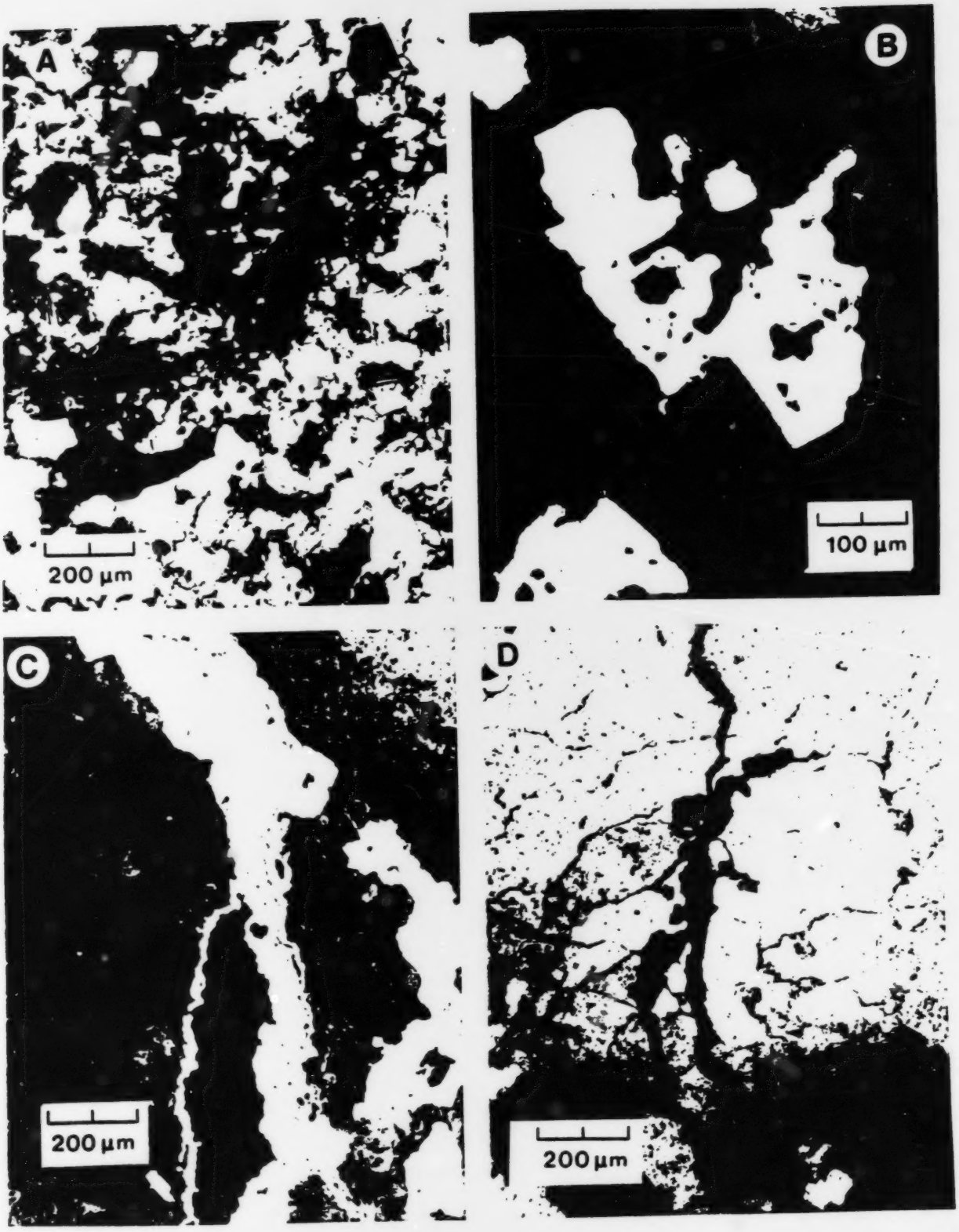

ASPLER FIG 7

ASPECT TABLE II-1-a

GOSSAN	SAMPLE	NTS/UTM	UNIT
1	17-3	65C/7, 149963	Tavani Fm
2A	18-5A	65/C9, 266098	Watterson Fm
2B	18-5B	65C/9, 266098	Watterson Fm
3A	20-8A	65C/8, 216967	K1
3B	20-8B	65C/8, 216967	K1
4A	23-1C	65C/9, 355109	Basement
4B	23-1F	65C/9, 355109	Basement
5	23-6	65C/9, 361128	Basement
6A	23-10B	65C/9, 347128	K2
6B	23-10D	65/C9, 347128	020 Diabase
6C	23-10E	65C/9, 347128	K2
6D	23-10G	65C/9, 347128	K2
7	24-3	65C/9, 379127	K1
8	24-11	65C/9, 381147	Tavani Fm
9	26-3A	65C/8, 343065	Ameto Fm
10	26-6C	65C/8, 345032	Watterson Fm
11	27-11	65C/9, 355099	K1
12	L-2-2	65C/9, 181069	Watterson Fm
13	L-2-6	65C/10, 163092	K1
14	L-4-3	65C/7, 156062	Watterson Fm
15	T-7-2A	65C/7, 108029	Watterson Fm
16	5-4-B	65C/9, 235086	Watterson Fm
17	29-3	65C/9, 337126	Basement
18	31-2A	65C/9, 334111	Watterson Fm

19	33-3B	65C/9, 300305	Basement
20	35-1	65C/8, 350007	Ameto Fm
21A	35-3A	65C/8, 355975	Ameto Fm
21B	35-3B	65C/8, 355975	Ameto Fm
22	39-17	65C/9, 399145	Watterson Fm
23	40-9	65C/9, 353208	Hurwitz H
24	41-4A	65C/9, 426213	Kinga Fm
25A	44-7A	65C/8, 219915	Watterson Fm
25B	44-7B	65C/8, 219915	Watterson Fm
25C	44-7C	65C/8, 219915	Watterson Fm
26	51-2	65C/7, 995974	Tavani Fm
27	T-23-2B	65C/7, 007868	K2

TABLE II-2-a

1 Quartz arenite with calcite cement. Random clusters of metamorphic pyrite transect detrital grains; hematite as rims and internal fracture fills to pyrite (Figs. 7A,B).

2A. Quartz vein cutting actinolite-bearing metacarbonate. Pyrite and hematite disseminated in quartz. Quartz veins folded/rotated about thrust-related fabrics.

2B Interlayered siltstone and actinolite-bearing metacarbonate.

3A Conglomerate with clasts of quartz arenite, granite, milky quartz. Pyrite and hematite in fractures.

3B Quartz vein cutting thrust/fold related fabrics in conglomerate. Marcasite and pyrite in fractures (Fig. 7D); hematite after sulphides.

4A Silicified pod within mafic volcanic

4B Mafic volcanic. Disseminated pyrrhotite, pyrite and chalcopyrite cut across actinolite alteration.

5 Mafic volcanic

6A Fractured arkose. Hematite after magnetite in fractures.

6B Diabase

6C Arkosic brittle fault gouge

6D Arkose

7 Conglomerate, metamorphic biotite in matrix. Sulphides along cleavage.

8 Quartz arenite.

9 Argillite with sulphide stain surrounding quartz veins.

10 Arkosic granulestone with disseminated hematite and hematite-lined fractures

11 Conglomerate

12 Recrystallized arkose cut by feldspar and quartz-filled veins with fracture fills of pyrite (altered to marcasite), arsenopyrite and hematite (Fig. 4C,D, 5). Disseminated pyrite.

13 Arkose

14 Arkose

15 Arkose cut by quartz veins.

16 Weakly alligned to randomly oriented actinolite and calcite mosaic with local sand-sized quartz and feldspar grains. Disseminated pyrrhotite and chalcopyrite cut across actinolite boundaries.

17 Mafic volcanic. Disseminated pyrrhotite with inclusions of chalcopyrite replacing actinolite; disseminated magnetite with hematite alteration.

18 Arkose with granule-sized granite and granoblastic polygonal quartz grains. Brittle fractures across grains filled with hematite (Fig. 6B)

TABLE II-26

19 Amphibolite gneiss

20 Argillite with randomly oriented biotite and cordierite. Pyrrhotite, chalcopyrite and pyrite replace cordierite and biotite (Figs. 4A, B). Disseminated magnetite with hematitic alteration.

21A Arkosic granulestone. Hematite along fractures.

21B Argillite with porphyroblasts of randomly oriented biotite. Magnetite with hematite alteration replacing biotite.

22 Arkosic granulestone with randomly oriented metamorphic actinolite, magnetite, hematite cement. Magnetite and hematite fill fractures across grain boundaries; replace actinolite and detrital grains (Fig. 6A).

23 Arkose with disseminated pyrite, chalcopyrite, magnetite, hematite.

24 Granoblastic polygonal quartz with muscovite growth defining planar fabric. Hematite in fractures.

25A Siltstone with randomly oriented porphyroblasts of actinolite and biotite. Disseminated magnetite cuts across actinolite boundaries; hematite in fractures.

25B Siltstone with randomly oriented porphyroblasts of actinolite and biotite. Disseminated magnetite with hematite alteration cuts across actinoloite grains.

25C Arkosic granulestone. Marcasite after pyrite replaces detrital grains (Fig. 6 C,D). Fractures across grain boundaries filled with pyrite and hematite; fractures in pyrite filled with magnetite (Fig. 7C).

26 Granoblastic polygonal quartz. Disseminated pyrite and chalcopyrite as random replacements of quartz and in fractures

27 Pebbly arkose. Disseminated pyrrhotite pyrite with inclusions of chalcopyrite replace granules of granoblastic polygonal quartz and metamorphic biotite. Hematite along fractures.

II-3-a

ELEMENT	Na	Sc	Cr	Fe	Co	Ni	Zn	As
DETECTION LIMIT	0.05 PCT	0.5 PPM	50 PPM	0.5 PCT	10 PPM	50 PPM	200 PPM	1 PPM
GOSSAN								
1	6.36	8.5	56	3.0	27	32	<100	320
2A	0.15	1.2	<20	0.6	<5	<20	140	212
2B	0.36	5.3	32	1.5	9	<20	120	20
3A	2.32	13.0	160	4.7	21	88	210	31
3B	0.10	1.2	<20	2.5	<5	<20	100	7.7
4A	1.40	11.0	21	3.9	17	<20	110	17
4B	2.03	44.1	230	12.0	32	32	180	17
5	1.40	38.5	670	7.7	51	200	140	4.0
6A	2.00	5.6	38	2.1	8	<20	150	46
6B	1.90	21.4	30	8.8	17	<20	120	39
6C	1.80	27.7	23	10.0	24	24	120	111
6D	2.06	22.1	30	9.3	13	22	130	99
7	1.60	26.1	150	7.4	31	70	240	5.7
8	4.56	9.1	90	5.5	100	140	<100	8.7
9	2.36	19.0	110	7.1	26	48	190	19
10	2.17	5.1	49	4.6	100	87	110	782
11	2.51	22.0	110	6.5	66	69	260	3.6
12	6.70	3.1	140	1.7	9	<20	150	>9,000
13	2.55	12.0	44	4.0	17	62	200	200
14	4.46	7.9	79	2.1	<5	<20	200	918
15	0.08	0.4	<20	0.2	<5	<20	110	39
16	0.56	8.8	76	6.8	35	25	<100	15
17	2.50	45.0	240	13.0	69	<50	<200	3
18	6.74	4.2	<50	2.0	<10	<50	<200	2

19	1.40	52.1	200	13.0	53	98	<200	<1
20	1.70	24.0	160	4.2	<10	<50	<200	3
21A	0.38	6.4	57	1.8	<10	<50	<200	<1
21B	0.91	6.9	<50	1.9	<10	<50	<200	<1
22	5.84	23.0	73	1.9	<10	<50	<200	3
23	1.70	14.0	93	4.0	<10	<50	<200	<1
24	0.08	0.9	<50	<0.5	<10	<50	<200	6
25A	4.60	10.0	96	3.1	<10	<50	<200	5
25B	3.10	17.0	110	3.6	<10	<50	<200	4
25C	7.66	6.0	100	6.9	<10	<50	<200	3
26	0.09	1.7	<50	1.8	<10	<50	<200	3
27	1.40	8.8	51	2.8	14	<50	<200	6

ELEMENT	Se	Br	Rb	Zr	Mo	Ag	Cd
DETECTION LIMIT	10 PPM	1 PPM	10 PPM	500 PPM	2 PPM	5 PPM	10 PPM
GOSSAN							
1	<5	<2	<14	<200	4	<2	<5
2A	<5	<2	<5	<200	<1	<2	<5
2B	<5	<2	<5	<200	<1	<2	<5
3A	<5	<2	81	220	2	<2	<5
3B	11	<2	<5	<200	1	4	<5
4A	<5	<2	90	<200	5	<2	<5
4B	<5	<2	<5	260	2	<2	<5
5	<5	<2	17	<200	<1	<2	<5
6A	<5	<2	69	270	2	<2	<5
6B	<5	<2	170	300	2	<2	<5
6C	<5	2.6	160	380	2	<2	<5
6D	<5	2.1	150	<200	2	<2	<5
7	<5	3.8	130	<200	2	<2	<5
8	<5	<2.0	<5	<200	8	<2	<5
9	<5	<2.0	250	230	<1	<2	<5
10	<5	2.8	48	<200	4	<2	<5
11	<5	<2.0	44	<200	<1	<2	<5
12	<5	14.0	8	<200	3	<2	<5
13	<5	<2.0	66	<200	2	<2	<5
14	<5	4.0	42	<200	2	<2	<5
15	<5	2.3	<5	<200	1	<2	<5
16	<5	<2.0	31	<200	2	<2	<5
17	<10	<1	44	<500	<2	<5	<10
18	<10	<1	54	570	4	<5	<10

19	<10	<1	30	<500	<2	<5	<10
20	<10	2	320	<500	<2	<5	<10
21A	<10	<1	88	<500	<2	<5	<10
21B	<10	<1	85	<500	<2	<5	<10
22	<10	26	36	<500	<2	<5	<10
23	<10	<1	77	<500	<2	<5	<10
24	<10	<1	<10	<500	<2	<5	<10
25A	<10	<1	95	<500	<2	<5	<10
25B	<10	<1	140	<500	<2	<5	<10
25C	<10	<1	<10	<500	<2	<5	<10
26	<10	<1	<10	<500	<2	<5	<10
27	<10	<1	170	<500	<2	<5	<10

ELEMENT	Sn	Sb	Te	Cs	Ba	La	Ce
DETECTION LIMIT	200 PPM	0.2 PPM	20 PPM	1 PPM	100 PPM	5 PPM	10 PPM
GOSSAN							
1	<100	1.6	<10	<0.5	<50	100	158
2A	<100	0.5	<10	<0.5	<50	2	<5
2B	<100	0.6	<10	<0.5	<50	32	57
3A	<100	1.0	<10	3.2	510	12	25
3B	<100	0.5	<10	<0.5	<50	3	<5
4A	<100	2.1	<10	1.6	1,100	16	32
4B	<100	4.2	<10	<0.5	67	5	11
5	<100	3.9	<10	1.0	51	2	<5
6A	<100	2.5	<10	<0.5	670	19	35
6B	<100	4.5	<10	<0.5	1,100	17	27
6C	<100	9.1	<10	<0.5	380	10	22
6D	<100	20.5	<10	<0.5	1,000	7	10
7	<100	1.4	<10	8.1	370	4	8
8	<100	1.1	<10	<0.5	<50	21	44
9	<100	1.3	<10	8.4	800	16	27
10	<100	1.1	<20	2.6	<50	6	14
11	<100	2.4	<10	2.2	290	11	21
12	<100	9.0	<29	<0.5	66	4	9
13	<100	1.0	<10	2.0	550	6	17
14	<100	1.6	<22	0.7	360	43	85
15	<100	0.4	<10	<0.5	<50	<2	<5
16	<100	5.2	<10	0.5	330	9	14
17	<100	2.5	<20	1	360	9	22
18	<100	1.0	<20	<1	480	23	54

19	<100	<0.2	<20	4	<100	<5	<10
20	<100	0.5	<20	5	400	100	240
21A	<100	0.3	<20	3	320	45	110
21B	<100	0.2	<20	3	430	55	130
22	<100	1.0	<20	<1	170	29	100
23	<100	0.7	<20	2	290	14	28
24	<100	0.6	<20	<1	<100	7	17
25A	<100	4.9	<20	1	100	26	64
25B	<100	4.5	<20	2	<100	46	100
25C	<100	2.1	<20	<1	<100	10	16
26	<100	0.3	<20	<1	<100	<5	<10
27	<100	0.4	<20	5	5,300	42	100

ELEMENT	Sm	Eu	Tb	Yb	Lu	Hf
DETECTION LIMIT	0.1 PPM	2 PPM	1 PPM	5 PPM	0.5 PPM	2 PPM
GOSSAN						
1	7.70	<2	<0.5	<2	0.3	11
2A	0.45	<1	<0.5	<2	<0.2	<1
2B	6.00	<1	0.7	2	0.3	3
3A	3.50	1	<0.5	<2	<0.2	5
3B	0.29	<1	<0.5	<2	<0.2	<1
4A	3.80	<1	0.6	2	0.4	6
4B	3.90	2	0.7	4	0.6	2
5	1.80	<1	<0.5	<2	0.3	<1
6A	3.90	<1	<0.5	<2	0.3	8
6B	4.10	<1	0.5	<2	0.4	3
6C	3.40	2	0.6	3	0.4	5
6D	2.70	1	<0.5	<2	0.3	3
7	1.60	<1	<0.5	<2	<0.2	4
8	4.70	2	0.6	3	0.3	5
9	3.20	2	0.5	3	0.4	6
10	2.80	<1	<0.5	2	0.3	6
11	3.40	<1	<0.5	2	<0.2	3
12	1.70	<1	<0.5	<2	<0.2	4
13	2.00	<1	<0.5	<2	0.3	3
14	6.40	<1	<0.5	<2	0.4	8
15	<0.20	<1	<0.5	<2	<0.2	<1
16	3.00	1	<0.05	<2	<0.2	5
17	4.0	<2	<1	<5	<0.5	4
18	3.6	3	<1	<5	<0.5	5

19	2.6	<2	<1	<5	<0.5	2
20	14.0	<2	<1	6	<0.5	11
21A	5.8	<2	<1	<5	<0.5	6
21B	7.1	<2	<1	<5	<0.5	9
22	10.0	<2	<1	<5	<0.5	5
23	1.5	<2	<1	<5	<0.5	6
24	0.6	<2	<1	<5	<0.5	<2
25A	3.5	<2	<1	<5	<0.5	5
25B	5.3	<2	<1	<5	<0.5	5
25C	2.1	<2	<1	<5	<0.5	3
26	<0.5	<2	<1	<5	<0.5	<2
27	5.3	<2	<1	<5	<0.5	9

ELEMENT	Ta	W	Ir	Au	Th	U
DETECTION LIMIT	1 PPM	2 PPM	100 PPB	5 PPB	0.5 PPM	0.5 PPM
GOSSAN						
1	1.3	37	<100	110	14.0	6.6
2A	<0.5	1	<100	6	0.6	0.2
2B	<0.5	1	<100	15	5.9	1.0
3A	0.5	2	<100	8	7.2	1.6
3B	<0.5	<1	<100	1,660	<0.2	<0.2
4A	0.8	2	<100	60	6.6	2.8
4B	<0.5	<1	<100	13	0.4	<0.2
5	<0.5	<1	<100	32	<0.2	<0.2
6A	<0.5	2	<100	3	8.6	1.4
6B	1.4	4	<100	8	2.8	0.7
6C	1.7	6	<100	7	3.7	2.4
6D	1.2	2	<100	8	2.6	0.6
7	<0.5	<1	<100	19	3.0	0.6
8	1.1	3	<100	4	13	3.3
9	1.9	2	<100	3	25.5	3.4
10	1.0	1	<100	<2	10.0	3.0
11	<0.5	<1	<100	2	2.0	0.6
12	<0.5	49	<100	<150	6.8	1.1
13	<0.5	1	<100	13	2.2	1.5
14	1.0	14	<100	8	12.0	3.3
15	<0.5	<1	<100	<2	0.3	<0.2
16	0.9	6	<100	24	13.0	3.3
17	<1	14	<100	160	1.0	<0.5
18	<1	11	<100	18	4.3	0.7

19	<1	<2	<100	9	<0.5	0.7
20	2	<2	<100	100	31.0	5.9
21A	<1	<2	<100	<5	11.0	2.1
21B	<1	<2	<100	<5	15.0	2.6
22	<1	<2	<100	<5	16.0	2.1
23	<1	<2	<100	14	14.0	2.7
24	<1	<2	<100	11	1.5	1.0
25A	<1	7	<100	<5	16.0	2.2
25B	<1	6	<100	<5	14.0	1.5
25C	<1	54	<100	<5	8.2	0.9
26	<1	<2	<100	<5	<0.5	<0.5
27	<1	<2	<100	<5	15.0	2.7